Telomerase activity is required for bleomycin-induced pulmonary fibrosis in mice

Tianju Liu,[1] Myoung Ja Chung,[1] Matthew Ullenbruch,[1] Hongfeng Yu,[1] Hong Jin,[1] Biao Hu,[1] Yoon Young Choi,[1] Fuyuki Ishikawa,[2] and Sem H. Phan[1]

[1]Department of Pathology, University of Michigan Medical School, Ann Arbor, Michigan, USA. [2]Laboratory of Cell Cycle Regulation, Department of Gene Mechanisms, Graduate School of Biostudies, Kyoto University, Kyoto, Japan.

In addition to its well-known expression in the germline and in cells of certain cancers, telomerase activity is induced in lung fibrosis, although its role in this process is unknown. To identify the pathogenetic importance of telomerase in lung fibrosis, we examined the effects of telomerase reverse transcriptase (TERT) deficiency in a murine model of pulmonary injury. TERT-deficient mice showed significantly reduced lung fibrosis following bleomycin (BLM) insult. This was accompanied by a significant reduction in expression of lung α-SMA, a marker of myofibroblast differentiation. Furthermore, lung fibroblasts isolated from BLM-treated TERT-deficient mice showed significantly decreased proliferation and increased apoptosis rates compared with cells isolated from control mice. Transplantation of WT BM into TERT-deficient mice restored BLM-induced lung telomerase activity and fibrosis to WT levels. Conversely, transplantation of BM from TERT-deficient mice into WT recipients resulted in reduced telomerase activity and fibrosis. These findings suggest that induction of telomerase in injured lungs may be caused by BM-derived cells, which appear to play an important role in pulmonary fibrosis. Moreover, TERT induction is associated with increased survival of lung fibroblasts, which favors the development of fibrosis instead of injury resolution.

Introduction

Telomeres consist of tandem hexanucleotide $(TTAGGG)_n$ repeats that cap the termini of eukaryotic chromosomes and play essential roles in maintenance of chromosomal stability and cell viability (1). The complex that is responsible for telomerase activity includes a reverse transcriptase that adds on telomeric repeats at the end of chromosomes using an RNA template. This telomerase core enzyme consists of the telomerase RNA (TR) component and a polypeptide that bears classical structural motifs and functional activities of a telomerase reverse transcriptase (TERT). The RNA component is constitutively expressed in both normal and cancerous tissues expressing telomerase activity, but can also be detected in cells and tissues lacking detectable telomerase activity (2, 3). Thus TR appears not to be the limiting factor in the expression of telomerase activity. This is in contrast to TERT, whose expression correlates with presence of telomerase activity, hence TERT is considered as the key determinant of induction of telomerase activity (4–6). Previous studies have shown that telomerase is only functional during embryonic development and in the germline of the adult organism, but not in normal adult somatic cells. Furthermore, cells of highly proliferative and periodically or continuously renewing tissues, such as cells of the hematopoietic system and the epidermis, exhibit telomerase activity (7, 8). However in addition to these normally or constitutively telomerase-positive cells and tissues, recent studies have also demonstrated significant induction of telomerase activity in normally telomerase-negative adult tissues when exposed to injury. For instance, telomerase activity is highly induced in a rodent model of pulmonary injury and fibrosis induced by bleomycin (BLM), where it is shown to be selectively induced in fibroblasts but not in differentiated myofibroblasts (9). The BLM-induced telomerase activity is inhibited by treatment of these cells with IL-4 or TGF-β1, which are known to induce expression of α-SMA and myofibroblast differentiation (10). Indeed it has recently been shown that suppression of telomerase activity is closely associated with myofibroblast differentiation, while induction of telomerase by bFGF inhibits α-SMA expression (11). However, the role of telomerase in myofibroblast differentiation remains unclear, nor is it clear whether the induction of telomerase is of importance in the pathogenesis of pulmonary fibrosis.

Additional potential methods by which telomerase could play a role in fibrosis are based on the ample evidence suggesting that telomerase may be important in regulation of cell proliferation (12, 13), apoptosis (14–16), and cell differentiation (17, 18). In cells that do express telomerase activity, its expression is intimately related to cell growth (12). Telomere shortening limits the replicative potential of organs and the lifespan of primary human cells in vivo during chronic diseases (13). Telomerase inhibition in human epidermoid tumor cell line A431 by a dominant-negative TERT mutant construct leads to chromosome damage, which in turn triggers apoptotic cell death (16). While inhibition of telomerase expression in progenitor cells is often regarded as a consequence of cell differentiation, these previous studies (8, 10, 11, 19) also indicate that the inhibition of telomerase activity could also serve as a prerequisite or initiator of the cell differentiation process.

Pulmonary fibrosis is characterized by increased extracellular matrix deposition and cellularity, especially with respect to fibroblasts at the site of active fibrosis. Myofibroblasts, with their characteristic α-SMA expression, arise de novo in fibrosis, and they are thought to be the primary source of heightened matrix and profibrogenic cytokine expression (20–23). Increased numbers and persistence of these cells may be the basis for disease progression

Nonstandard abbreviations used: BLF, lung fibroblasts from BLM-treated mouse; BLM, bleomycin; CHX, cycloheximide; HYP, hydroxyproline; IPF, idiopathic pulmonary fibrosis; NLF, lung fibroblasts from saline-treated mouse; PDS, plasma-derived fetal bovine serum; PI, propidium iodide; TERT, telomerase reverse transcriptase; TR, telomerase RNA.

Conflict of interest: The authors have declared that no conflict of interest exists.

Citation for this article: *J. Clin. Invest.* **117**:3800–3809 (2007). doi:10.1172/JCI32369.

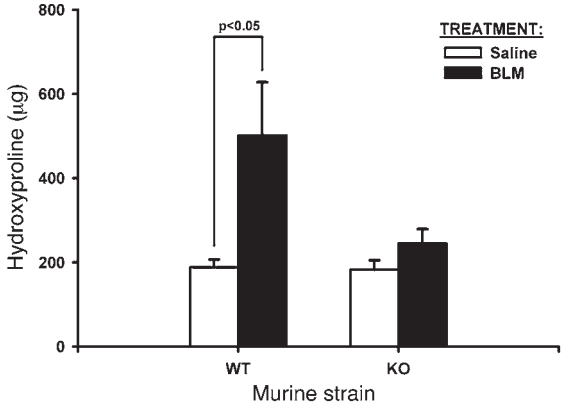

Figure 1
Effects of BLM treatment on lung HYP content. Whole-lung homogenates from the indicated strains were collected at day 21 after BLM or saline administration as indicated. Results (mean ± SEM) are expressed as μg per lung. $n = 5$ per group.

instead of resolution, resulting in end-stage disease and a fatal outcome (24, 25). Hence, understanding the origins, expansions, and possible fates of these activated fibroblasts is important to uncover the fibrotic pathogenesis. While telomerase activity is thought to be important for cancer cell propagation and its essentially unlimited replicative potential, the role of telomerase induction in the injured and fibrotic lung is unknown despite the demonstration of the telomerase-expressing fibroblast phenotype present during active fibrosis (9, 10). Here we investigated the in vivo role of telomerase in lung injury and fibrosis by comparing the responses to lung injury of TERT$^{-/-}$ mice and their WT counterparts. The findings using BLM to induce pulmonary fibrosis revealed that TERT deficiency caused reduced fibrosis and myofibroblast differentiation, which was restored by transplantation of WT BM to the TERT$^{-/-}$ mice.

Results

BLM-induced pulmonary fibrosis was reduced in TERT$^{-/-}$ mice. TERT$^{-/-}$ mice were generated as previously described (26). To evaluate the amplitude of BLM-induced lung fibrosis in TERT$^{-/-}$ mice, lung collagen content was compared in TERT$^{-/-}$ and WT mice by hydroxyproline (HYP) analysis at day 21 after BLM administration. The results showed that pulmonary fibrosis was significantly reduced in TERT$^{-/-}$ mice compared with WT mice (Figure 1). This marked reduction in biochemically assessed fibrosis was confirmed by morphological analysis of lung tissue sections. The results showed that while the lungs from BLM-treated WT mice exhibited typical severe pulmonary fibrosis, characterized by increased cellularity, loss of normal alveolar architecture, and thickening of alveolar septa, the lungs from BLM-treated TERT$^{-/-}$ mice had substantially less fibrosis, with more patchily distributed lesions that were much smaller in size and extension (Figure 2). Saline-treated control lungs showed no morphological abnormalities in both WT and TERT$^{-/-}$ mice, indicating that TERT deficiency did not impair normal lung development. Thus both biochemical and morphological assessment indicated that TERT deficiency resulted in significantly reduced BLM-induced pulmonary fibrosis.

TERT deficiency reduced genesis of myofibroblasts in pulmonary fibrosis. Previously, alterations in telomerase expression were found to affect myofibroblast differentiation (11). To investigate whether TERT deficiency also affects the genesis of myofibroblasts in pulmonary fibrosis in vivo, lung α-SMA expression, a marker of myofibroblast differentiation, was analyzed by real-time PCR at day 7 after BLM-induced lung injury. As expected, BLM treatment in WT mice caused a significant increase (>2-fold over saline-treated controls; $P < 0.001$) in lung α-SMA mRNA levels; conversely in TERT$^{-/-}$ mice, a slight, nonsignificant reduction was noted in the BLM-treated group relative to the saline-treated control group (Figure 3A). Consistent with these differences in lung tissue mRNA levels, α-SMA protein expression analyzed by Western blotting showed similar differences between the various groups (Figure 3B). Protein levels in WT mice were significantly higher (almost 2-fold increase; $P < 0.001$) in the BLM-treated compared with the saline-treated group, but in TERT$^{-/-}$ mice were slightly decreased in the BLM-treated group and not significantly different from saline-treated controls. This pattern of differences in α-SMA expression was also reflected in fibroblasts isolated from these lungs (data not shown). These findings indicated that myofibroblast differentiation as determined by α-SMA expression was significantly reduced in TERT$^{-/-}$ compared with WT mice.

Because BLM is also known to cause DNA strand scission and damage (27–29), the protective effect of TERT deficiency in the BLM model may be specific only for genotoxic injury–induced pulmonary fibrosis. To examine this possibility, DNA damage was evaluated in the BLM model using the Comet assay. The results showed that lung cell samples from both WT and TERT$^{-/-}$ mice at day 1 after BLM treatment did not exhibit comet tails (Figure 4). In contrast, positive control samples from H_2O_2-treated cells induced marked comet tails, as expected. Lung cells from mice at day 7 after BLM treatment and primary cultured isolated fibroblasts from mice at days 1 and 7 after BLM treatment also showed no evidence of DNA damage (data not shown). Thus, BLM treatment in vivo to induce pulmonary fibrosis, at the indicated dose (1.5 U/kg body weight), showed no evidence of genotoxicity using this assay. This made it unlikely that TERT deficiency protects only fibrosis resulting from a genotoxic insult.

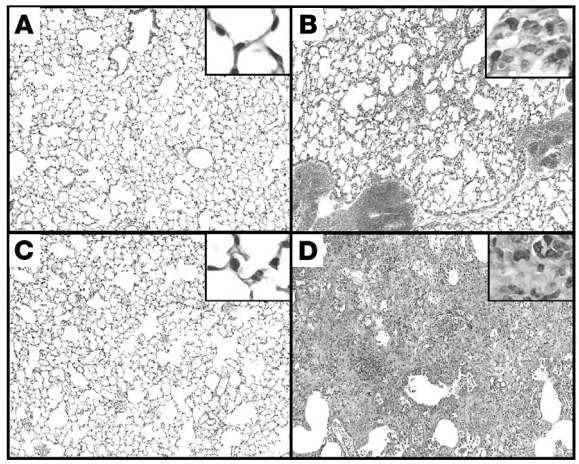

Figure 2
Histopathological changes of the lung tissues at day 21. Representative H&E-stained lung tissue sections from WT and TERT$^{-/-}$ mice treated by BLM or saline are shown, with higher-magnification views in insets. (**A**) Saline-treated TERT$^{-/-}$. (**B**) BLM-treated TERT$^{-/-}$. (**C**) Saline-treated WT. (**D**) BLM-treated WT. Original magnification, ×100; ×400 (insets).

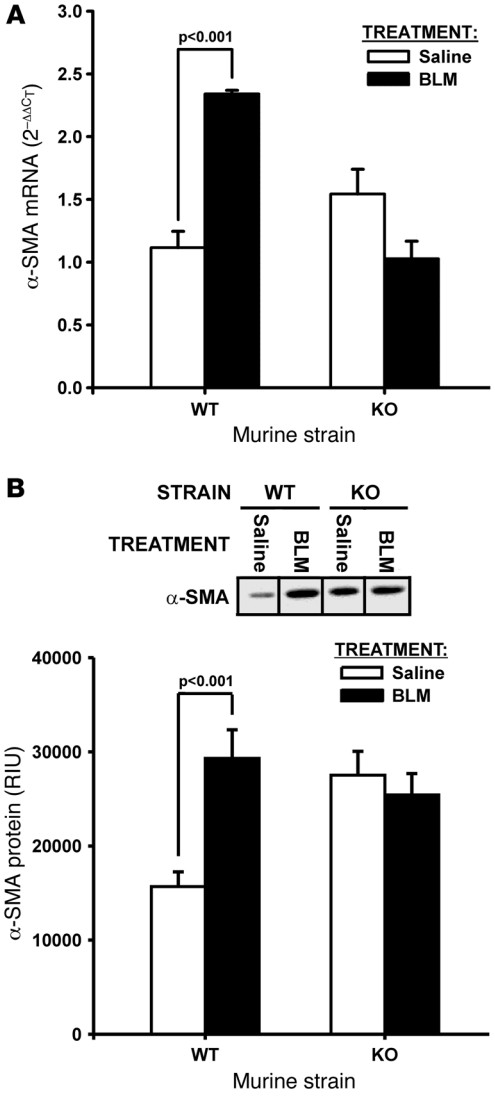

Figure 3
Effects of BLM on lung α-SMA expression. Lung total RNA and protein were isolated from the indicated mice at days 7 and 21 after BLM or saline treatment, respectively. (**A**) α-SMA mRNA was detected by real-time PCR, and results were expressed as $2^{-\Delta\Delta CT}$, with GAPDH used as the endogenous control and the level in saline-treated WT mice as reference. Data are mean ± SEM. $n = 3$ per group. (**B**) α-SMA protein was detected by Western blotting and expressed as relative integration units (RIU) after measurement of net intensity of scanned bands. The same amount (5 μg) of tissue protein was loaded on the 12% SDS-polyacrylamide gel and blotted with anti–α-SMA antibody. A typical blot from 3 independent experiments and the quantitative plot are shown.

To confirm this finding, the effect of TERT deficiency was studied in another model that is not known to be induced by a genotoxic insult, namely, one induced by FITC. While this model did not cause as severe a fibrosis as did BLM, the results did show a significant increase (~68%; $P < 0.05$) in lung type I collagen in WT FITC-treated mice (Figure 5). In contrast, lung type I collagen content was not significantly altered by FITC-treatment in TERT$^{-/-}$ mice, reminiscent of the protection against BLM-induced fibrosis in these mice. These findings suggested that TERT deficiency also has a protective effect against FITC-induced pulmonary fibrosis, and thus the protective effect of TERT deficiency is not specific only to the BLM model.

TERT deficiency affected lung fibroblast proliferation and apoptosis. To explore the possible mechanisms by which fibrosis was reduced in TERT$^{-/-}$ mice, the effects of TERT deficiency on lung fibroblast proliferation and apoptosis were analyzed to determine whether reduction in fibroblast numbers could be a factor. The cell proliferative responses of lung fibroblasts isolated from BLM- or saline-treated mice (BLF and NLF, respectively) at day 14 were determined as described in Methods. The results showed that WT BLF proliferated at a significantly higher rate (>2-fold increase) than did WT NLF, whereas KO BLF proliferation was not significantly different from KO NLF (Figure 6). Both the KO NLF and the KO BLF proliferation rates were not significantly different from the WT NLF rate, but were all significantly lower than the WT BLF rate. Thus TERT deficiency did not significantly affect proliferation in normal lung fibroblasts, but appeared to impair the emergence of an activated fibroblast population with higher proliferative rate in response to lung injury and remodeling.

The effect of TERT deficiency on fibroblast survival was also analyzed by assessing the response to a known apoptotic stimulus (5 ng/ml TNF-α with 500 ng/ml cycloheximide [CHX]). The apoptotic response to TNF-α was evaluated by TUNEL staining in the same lung fibroblast populations described above. The results showed that in the absence of apoptotic stimuli, both WT NLF and WT BLF exhibited low levels of apoptotic cells (<4%), which were significantly lower than the levels in KO NLF (7.6%) or KO BLM (20.3%; Figure 7A). Treatment with TNF-α caused an increase in the apoptotic rate in all cells, but the increase was significantly higher in both the KO NLF (21.5%; $P < 0.001$) and the KO BLF cells (47.8%; $P < 0.001$) compared with their respective untreated groups and with both treated WT groups ($P < 0.05$). Analysis of apoptosis using flow cytometric assessment of annexin V–FITC–propidium iodide (annexin V–FITC–PI) staining confirmed the markedly higher apoptotic potential of lung fibroblasts from control and BLM-treated TERT$^{-/-}$ mice (Figure 7, B–I). Consistent with the data shown by TUNEL staining, the apoptotic cells in the absence of apoptotic stimuli were 1.86% and 2.96% in WT NLF and WT BLF, respectively, whereas the corresponding values in KO NLF and KO BLF were more than 2-fold higher at 7.76% and 7.74%, respectively. Treatment with TNF-α caused increases in apoptosis in all cell groups, which again were almost 3-fold higher in the KO compared with the WT groups. The results of these apoptosis experiments indicated that, relative to cells from WT mice, lung fibroblasts from TERT$^{-/-}$ mice are substantially more susceptible to apoptotic stimuli, especially in cells from injured lungs undergoing fibrosis. Thus, in addition to reduced proliferative capacity, the increased susceptibility to apoptosis may affect the survival of these cells and result in reduced cell numbers in TERT$^{-/-}$ mice.

Contribution of BM-derived cells to lung telomerase induction and fibrosis. Previously, GFP BM chimera mice have been used to determine the presence of BM-derived fibroblast-like cells in BLM-injured lung as well as which are TERT positive (30). To investigate the possibility that BLM-induced lung telomerase expression may be caused by recruitment of these BM-derived cells, and to assess their role in fibrosis, BM chimera WT and TERT$^{-/-}$ mice, transplanted with corresponding TERT$^{-/-}$ and WT BM, were created and analyzed for

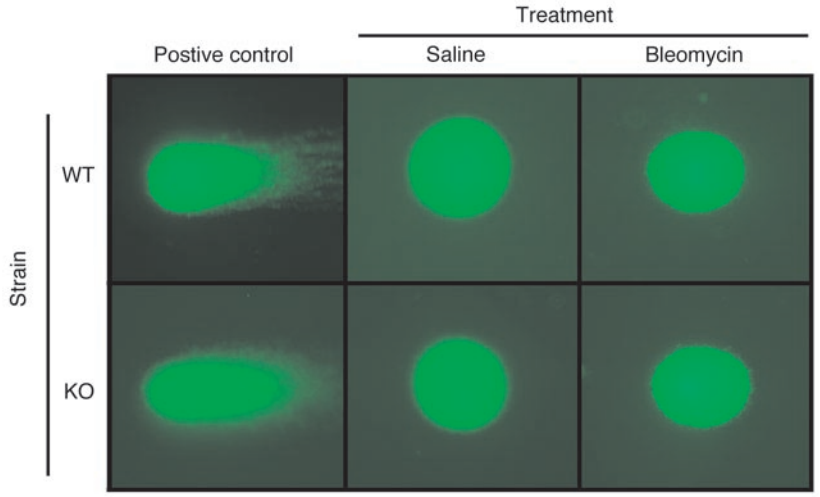

Figure 4
Assessment of BLM genotoxicity. DNA damage was visualized by SYBR green I staining of lung cellular DNA after single-cell electrophoresis. Damaged DNA fragments exhibited comet-like tails in cells exposed to H_2O_2, as shown in positive controls. Representative lung cells from whole-lung homogenates of WT or TERT$^{-/-}$ mice treated with BLM or saline are shown. Original magnification, ×400.

effects on BLM-induced lung telomerase and fibrosis. Sham controls consisted of TERT$^{-/-}$ and WT mice receiving TERT$^{-/-}$ and WT BM, respectively. The results showed that transplantation of WT BM into TERT$^{-/-}$ mice reconstituted BLM-induced lung telomerase activity to a level indistinguishable from that in WT mice (Figure 8A). Interestingly, transplantation of BM from TERT$^{-/-}$ mice to WT mice caused a marked reduction in BLM-induced lung telomerase induction. These findings showed that BM-derived cells were the main source of induced lung telomerase activity in BLM-induced pulmonary fibrosis.

In view of the ability of BM-derived cells to reconstitute the induction of lung telomerase activity by BLM treatment in TERT$^{-/-}$ mice, the same BM chimera mice were analyzed for responses to BLM-induced pulmonary fibrosis. Analysis of lung HYP content on day 21 after BLM treatment showed the expected increase in sham-transplanted WT mice relative to saline-treated controls, which was significantly higher than that in sham-transplanted TERT$^{-/-}$ mice (Figure 8B). However, as in the case of telomerase induction (Figure 7A), transplantation of WT BM to TERT$^{-/-}$ mice reconstituted the WT response to BLM-induced fibrosis, while transplantation of BM from TERT$^{-/-}$ mice to WT mice reduced the response relative to that in sham-transplanted WT mice.

Because myofibroblast differentiation correlated with the fibrotic response to BLM, these groups of BM chimera mice were also analyzed for BLM-induced alterations in lung α-SMA protein levels by Western blotting. Consistent with the whole-lung HYP changes, the lung α-SMA expression was similarly altered in the various groups of mice (Figure 8C). Thus transplantation of WT BM to TERT$^{-/-}$ mice caused α-SMA induction by BLM to be at a level comparable to that in WT mice, while the converse transplantation of BM from TERT$^{-/-}$ mice to WT mice ablated this response. Taken together, these findings suggested that lung telomerase induction from BM derived cells in response to BLM treatment was important for the pathogenesis of pulmonary fibrosis.

Discussion

The common feature characteristic of idiopathic pulmonary fibrosis (IPF) is the presence of fibroblastic foci, areas rich in mesenchymal cells, including increased numbers of fibroblasts and fully differentiated myofibroblasts. This population of cells is the key cellular source of extracellular matrix, and is heterogeneous with respect to a number of key phenotypes (31, 32). The de novo emergence or genesis of α-SMA–expressing myofibroblasts is well described in lung fibrotic lesions in both human and animal model studies (20, 23). More recently, a telomerase-expressing fibroblast phenotype without appreciable α-SMA expression has been isolated from lungs of rats with BLM-induced pulmonary fibrosis during active fibrosis (9, 24). Telomerase is initially known to be expressed by cells with high proliferative capacity, and later studies also indicate that the overexpression of TERT subunit promotes stem cell proliferation without changes in telomere length (13, 33–35). There is evidence that this telomerase-expressing fibroblast phenotype in fibrosis could be differentiated to the myofibroblasts by certain cytokines such as TGF-β1 and IL-4, suggesting that this phenotype may be an intermediate toward terminal differentiation to the myofibroblast phenotype (10, 11). However, in view of the heterogeneity of the lung fibroblast populations noted previously, it remains uncertain whether this differentiation is occurring in the same cell or cell type or is the result of selection for one or more subpopulations induced by the cytokine treatment. Moreover, the role of this lung injury–induced telomerase-expressing fibroblast phenotype in fibrosis is as yet undefined.

To begin addressing some of these issues, the effects of TERT deficiency on pulmonary fibrosis, genesis of the myofibroblast, and fibroblast survival were examined using the rodent BLM model. Our

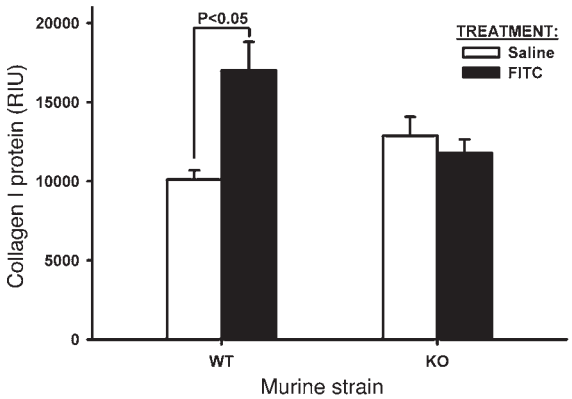

Figure 5
Effects of FITC on lung collagen. WT and TERT$^{-/-}$ mice were treated as indicated, and lung tissue homogenates were prepared for analysis of type I collagen by Western blotting. Equal amounts of protein (20 μg) were loaded per lane, and the resulting blot was scanned and digitized for quantitative analysis of band intensity. Results are mean ± SEM. n = 5 per group.

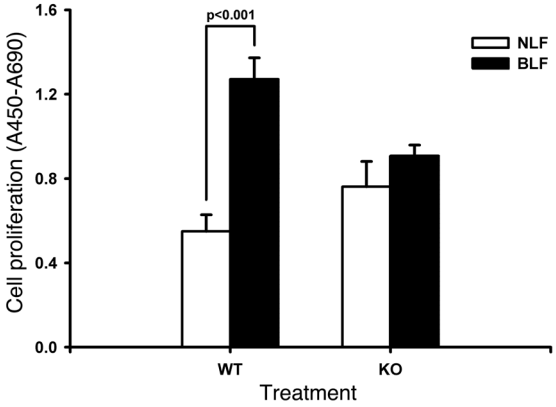

Figure 6
Effects of BLM on fibroblast proliferation. BLF and NLF were isolated from the indicated mice after BLM or saline treatment (cultured in DMEM supplemented with 10% PDS, 10 ng/ml EGF, and 5 ng/ml PDGF), respectively. Cell proliferation was determined using the WST-1 assay; results (mean ± SEM) are expressed as the difference between the absorbance at 450 nm and that at 690 nm. $n = 5$ per group.

data indicated that BLM induced much less fibrosis in TERT$^{-/-}$ mice relative to that in WT animals, as assessed by lung collagen content, histopathology, and α-SMA expression in the lung. BLM-induced lung injury causes increased numbers of fibroblasts and myofibroblasts in the lung associated with fibrosis, and the fibroblasts isolated from such lungs show increased intrinsic proliferative capacity (23, 36). In view of the importance of telomeres in determining cell replicative potential and the role of telomerase in maintaining them, a potential mechanism for the protection from fibrosis afforded by TERT deficiency may be the result of a reduction in fibroblasts in the TERT$^{-/-}$ mice. The noted reduction in cellularity in the lung histopathology of TERT$^{-/-}$ mice would be consistent with such a possibility. Such a reduction may be caused by reduced proliferative potential and/or increased rates of cell death, perhaps in response to

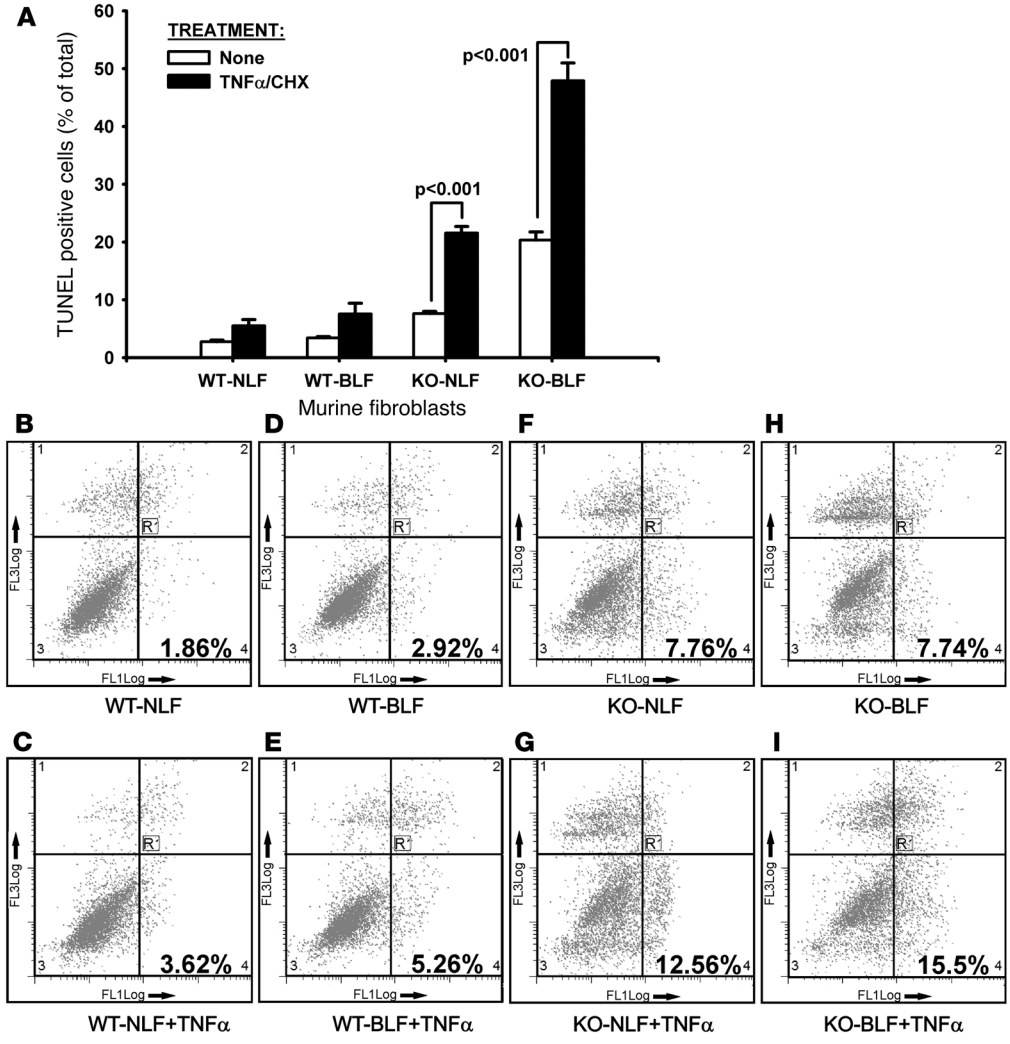

Figure 7
Effects of BLM on fibroblast apoptosis. Apoptosis of lung fibroblasts were detected by TUNEL staining (**A**) and flow cytometry after annexin V–FITC staining (**B**–**I**). (**A**) Lung fibroblasts from the indicated groups were cultured in 4-well chamber slides and treated with buffer only or TNF-α plus CHX. Apoptosis was analyzed by TUNEL staining after 4 hours of treatment: 500 cells in randomly selected high-power fields (original magnification, ×400) were counted, and apoptotic cells were expressed as a percentage of the total cells counted. Data are mean ± SEM. $n = 3$ per group. (**B**–**I**) For annexin V analysis, the cells were treated similar to that described above in 60-mm dishes and trypsinized after TNF-α and CHX treatment for annexin V–FITC and PI staining. The *x* axis (FL1) reflects annexin V–FITC fluorescence; the *y* axis (FL3) reflects PI fluorescence. Early apoptotic (annexin V–FITC–positive) cells appear in the lower right quadrant of the dot plot. A typical result from 3 independent experiments is shown.

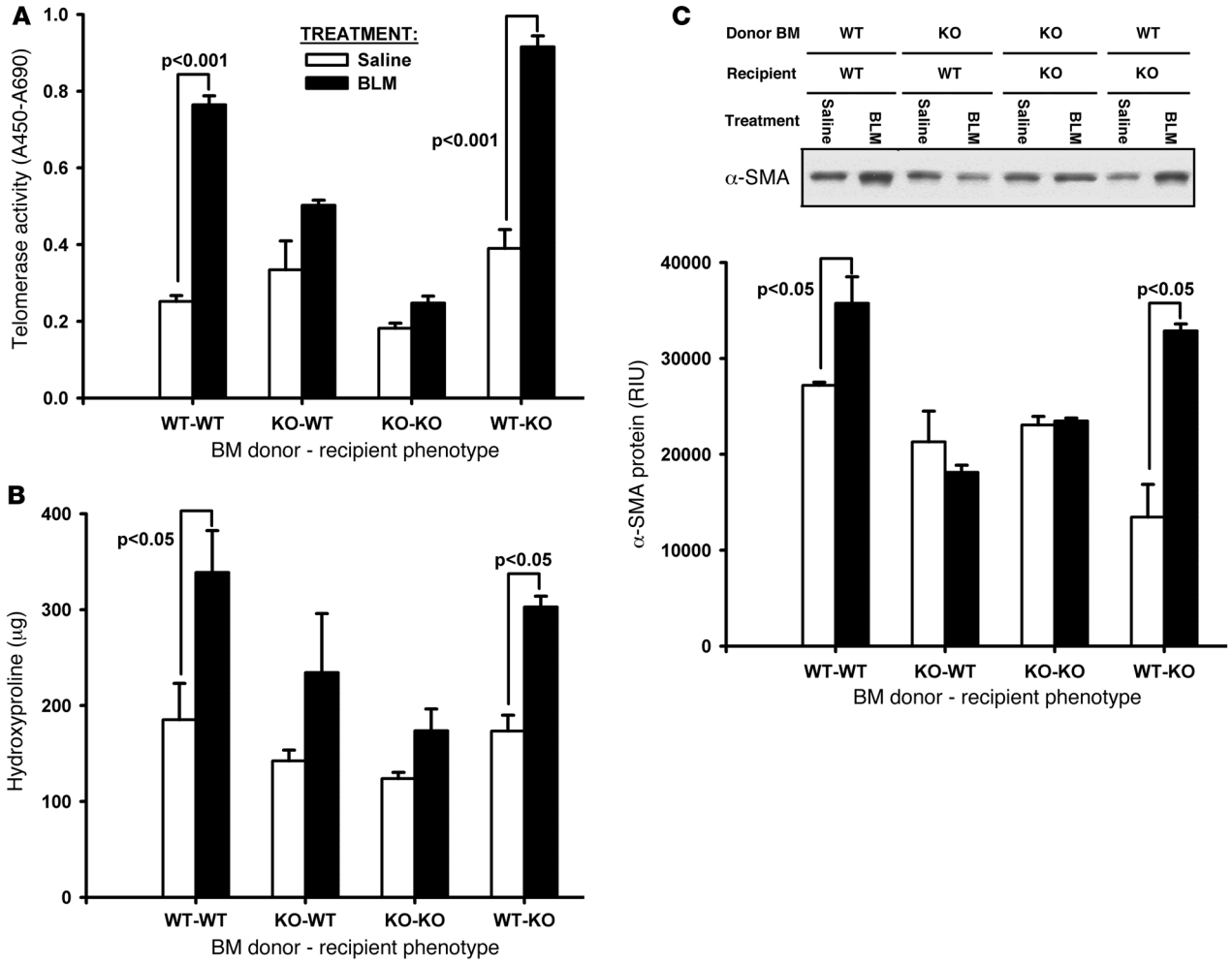

Figure 8

Effects of BM transplantation on lung telomerase and fibrosis. BM chimera mice were generated as described in Methods by transplanting WT BM into TERT$^{-/-}$ and TERT$^{-/-}$ BM into WT mice (WT-KO and KO-WT, respectively). BM transplantation from TERT$^{-/-}$ to TERT$^{-/-}$ or WT to WT mice were used as sham controls. Whole-lung lysates were collected at day 21 after BLM or saline treatments. (**A**) Lung telomerase activity was measured by TRAP-based ELISA, and results were expressed as the difference between absorbance at 450 nm and that at 690 nm. (**B**) Lung collagen content was analyzed with HYP assay. (**C**) α-SMA expression was detected by Western blotting with equal amounts (5 μg) of protein loaded per lane. A typical blot and the quantitative plot are shown. Data are mean ± SEM. *n* = 5 (BLM); 3 (saline).

apoptotic stimuli. A large body of evidence indicates that telomerase is associated with cell proliferation and apoptosis. For example, conditional transgenic induction of TERT in mouse skin epithelium causes a rapid transition from the resting phase of the hair follicle cycle to the active phase by causing proliferation of quiescent, multipotent stem cells in the hair follicle bulge region (13). It is noteworthy that this effect does not require the telomerase RNA component, suggesting that TERT can promote proliferation of resting stem cells through a noncanonical pathway. In contrast, the pathologies that occur in the telomerase-deficient mouse model are accompanied by a reduction in proliferative potential or increased apoptosis in the affected tissues (37–39). In one of these studies, TR deficiency–associated telomere shortening was coupled with attenuation in cardiac myocyte proliferation but increased apoptosis (39). In agreement with these observations, other studies showed cell proliferation failures in rapidly dividing tissues such as the hematopoietic system and reduced life span in TR-deficient mice (40, 41).

In this report, to seek out the possible mechanisms for the noted reduction in pulmonary fibrosis as a consequence of TERT deficiency, cell proliferation and apoptosis were examined in lung fibroblasts isolated from BLM- or saline-treated TERT$^{-/-}$ mouse lungs for comparison with those from similarly treated WT mice. Our findings showed that significantly lower proliferation and higher apoptosis rates were induced in lung fibroblasts from BLM-treated TERT$^{-/-}$ mice compared with cells isolated from comparably treated WT mice. Thus telomerase deficiency may provide protection from pulmonary fibrosis by reducing lung fibroblast proliferative potential but increasing susceptibility to apoptosis. These effects would thus result in reduced fibroblast numbers typically found in fibrotic lesions. Previously, siRNA-mediated repression of TERT in a human bladder cancer cell line was reported to downregulate EGFR expression, suggesting a potentially new function of TERT in the regulation of EGFR-stimulated proliferation (35). There is evidence that EGFR or PDGFR are involved

in the proliferation and activation of myofibroblasts. The blockade of autophosphorylation of the EGFR or PDGFR by tyrosine inhibitors have been shown to suppress fibroblast proliferation and reduce fibrosis in a rat model of pulmonary fibrosis (42). The decrease of such proliferation-related growth factors may be a potential mechanism for reduced proliferation of fibroblasts in BLM-induced lung injury in TERT$^{-/-}$ mice.

Because BLM also has an effect on DNA damage (27–29), this protective effect of TERT deficiency may be specific to fibrosis induced by genotoxic injury. However, induction of fibrosis by the indicated dose of BLM (30 μg per 20-g mouse) did not cause detectable genotoxic injury using the standard Comet assay. This is not unexpected, because it is unlikely that the in vivo dose used would cause DNA damage to cells to the degree achieved by in vitro doses (>20 μg/ml) (27). Moreover, 100 mg/kg of BLM is required in vivo to induce DNA damage in liver of mice (29), which would be greater than 65-fold the dose used in this study for induction of pulmonary fibrosis. Thus it is unlikely that the protective effect of TERT deficiency would be specific to fibrosis due to a genotoxic insult. Furthermore, protection was also seen in another model induced by FITC, which is not known to be associated with genotoxic insult. Thus protection by lack of TERT is not specific to the BLM model or related to genotoxic-associated injury.

Given the association of telomerase expression with stem cells and the recent description of BM derivation of TERT-expressing fibroblasts in the BLM model (30), the contribution of BM-derived cells to the induction of lung telomerase and fibrosis was evaluated. Using BM chimera WT and TERT$^{-/-}$ mice transplanted with BM from corresponding TERT$^{-/-}$ and WT mice, the studies revealed that BLM-induced lung telomerase activity was rescued in TERT$^{-/-}$ mice by transplantation with WT BM. The data also demonstrated that the restored telomerase was sufficient to restore pulmonary fibrosis in this model. Moreover, the converse BM chimera WT mice transplanted with BM from TERT$^{-/-}$ mice revealed a significant reduction in lung telomerase induction and fibrosis. Thus the BLM-induced lung telomerase activity and fibrosis were dependent on the recruitment of BM-derived cells, which affected lung myofibroblast differentiation, fibroblast proliferation, and apoptosis susceptibility. While the focus in this study was on the telomerase-expressing fibroblast, the findings cannot rule out the involvement of additional BM-derived cell types that are capable of expressing TERT. The precise nature or phenotype of these BM-derived cells require further elucidation in future studies.

It is well established that ectopic expression of TERT or reintroduction of a telomerase RNA component transgene into TERT$^{-/-}$ ES cells can reconstitute robust telomerase activity and original growth rates (43–46). Transfection of TERT into fibroblasts results in telomere length elongation and extension of the in vitro replicative life span (47, 48). The reconstituted telomerase was shown to rescue the expression levels of keratinocyte growth factor, IGF-II, and heparin-binding EGF in senescent human fibroblasts (49). The restoration of fibrosis induction by BLM in this study might also be explained by recovery of fibroblast proliferation rate and the expansion of life span, and thus rescue the expression of proliferation-related growth factors.

In the present study, it is noteworthy that although the BLM-induced telomerase activity and fibrosis were much lower in TERT$^{-/-}$ mice than in BLM-treated WT mice compared with their respective controls, the basal levels of lung α-SMA gene expression were higher in saline-treated TERT$^{-/-}$ mice than in WT mice ($P < 0.05$). These observations are consistent with a previous study showing that the induced loss of telomerase activity in cultured rat lung fibroblasts is closely associated with myofibroblast differentiation and possibly functions as a trigger for such differentiation (11). Conversely, increased expression of telomerase by bFGF suppresses myofibroblast differentiation. A recent observation indicates that BM-derived precursor cells could serve as a source for telomerase-expressing fibroblasts in this model of pulmonary fibrosis (30). Given that (a) proliferating collagen-expressing fibroblasts can differentiate into myofibroblasts and promote fibrosis and (b) TERT-positive fibroblasts could be differentiated into myofibroblasts when they lose telomerase activity, the reduced fibrosis in TERT$^{-/-}$ mice may be caused by the migration of TERT$^{-/-}$ BM precursor cells with significantly reduced ability to survive. This reduced survival results in reduced overall fibroblast numbers and subsequent fibrosis.

Recent human studies of familial IPF, however, suggest an association between certain heterozygous mutations in TERT or TR and IPF in these families (50, 51), with the implication that shortened telomeres caused by deficiency in telomerase activity may play a role in disease pathogenesis. Although these mutations are associated with shortened telomeres, the extent of shortening does not significantly correlate with development of IPF. Furthermore, some family members with these mutations and significant telomere shortening did not have IPF at the time of the study. But decreased telomere length associated with these mutations suggests a potential role in the pathogenesis of IPF, such as by decreasing the regenerative capacity of alveolar epithelial progenitors. However, it is unclear whether decreased telomere length would impair the proliferation of the type II pneumocyte or its differentiation to the type I pneumocyte, for example. Nevertheless, these findings in familial IPF indicate complex phenotypes, depending on the degree and type of telomerase deficiency, that may not be directly dependent on the extent of telomere shortening because telomere shortening and/or TERT or TR mutations per se are insufficient to cause pulmonary fibrosis. As the authors suggest, the interaction with other factors (e.g., smoking) may be necessary to induce IPF. In contrast to these human studies, the results reported here in TERT$^{-/-}$ mice would seem to suggest that the role of TERT is essential for pulmonary fibrosis induced by BLM, instead of having a protective effect. While it is likely that telomere length would be decreased in TERT$^{-/-}$ mice, especially in the later generations, this appears to be associated with impairing BLM-induced fibrosis instead of promoting it. Interestingly, however, this impairment was corrected by WT BM transplantation, indicating that it is the TERT in BM-derived cells that seems to be important in fibrosis. The basis for this apparent discrepancy between human familial IPF and this murine model of fibrosis is unclear, but may be related to different pathogenic mechanisms and/or species differences related to telomere lengths and their pathophysiological significance. Additionally, there is some uncertainty with respect to the possibility of additional roles for TERT beyond the mere maintenance of telomere length. TERT is primarily responsible for the catalytic activity of telomerase and is not required for other vital functions, such as having a structural role at the telomeres. Telomeric G-tails are essential for the higher-order telomere structure, and these have been found to be produced by telomerase-independent mechanisms in mice (26) as well as in human and yeast cells (52, 53). While telomere length maintenance is dependent on TERT expression (13, 35), additional

roles on cell functions, such as survival, growth, and proliferation, have not been excluded, and in fact are strongly suggested by the data reported in the present study.

In summary, the current report showed that TERT deficiency reduced BLM-induced mouse pulmonary fibrosis and myofibroblast differentiation, which were also associated with decreased lung fibroblast proliferation rate and increased susceptibility to apoptosis. The restoration of telomerase activity in TERT$^{-/-}$ mice by WT BM transplantation rescued BLM induction of lung telomerase activity and fibrosis, indicating the importance of BM-derived precursor cells capable of expressing TERT in the pathogenesis of pulmonary fibrosis. Further studies are necessary to probe the origin and nature of the BM-derived lung TERT-positive cells and the mechanism by which they participate in fibrosis.

Methods

Animals and induction of pulmonary fibrosis. C57BL/6 mice were purchased from The Jackson Laboratory. TERT$^{-/-}$ mice on C57BL/6 background were produced as previously described (26). Briefly, a 4-kb region containing exons γ, δ, and ε was replaced by neomycin resistance gene *neo*. Exon γ codes for part of motif A of the mTERT protein (amino acids 701–753 of mTERT). The first-generation mTERT$^{-/-}$ mice were fertile and did not show any noticeable gross or microscopic abnormality during early generations (G1 and G2). mTR expression levels were essentially same in WT and mTERT$^{-/-}$ mice. All tissue cells derived from mTERT$^{-/-}$ mice lacked telomerase activity, which suggests that mTERT is the only gene encoding the telomerase catalytic subunit. Telomeric DNA in mTERT$^{-/-}$ mice has G-strand 5′-overhangs, indicating that these telomeric 5′-overhangs are produced by telomerase-independent mechanisms. These mice were propagated at the University of Michigan for these studies. G1–G3 mTERT$^{-/-}$ mice were used for these studies.

For induction of BLM-induced pulmonary fibrosis, BLM (Blenoxane) was dissolved in sterile PBS and instilled endotracheally at a dose of 1.5 U/kg body weight on day 0 as previously described (54). Control groups received the same volume of sterile PBS only. Mice (n = 3–5) were randomly assigned to each of the indicated treatment groups. At the indicated time points after BLM treatment, the mice were sacrificed, and their lungs were harvested rapidly. Where indicated, the lung tissue samples were immediately placed in TRIzol reagent (Invitrogen) for total RNA isolation or in lysis buffer (50 mM Tris.Cl, pH 7.5, and 1% Nonidet P-40) for protein analysis. For histopathological analysis, 21 days after BLM injection the lungs were formalin-fixed and stained with routine H&E, as previously described. FITC-induced pulmonary fibrosis was performed as previously described (55). Briefly, 20 mg FITC (Sigma-Aldrich) was dissolved in 10 ml sterile PBS, vortexed extensively, and followed by 30 seconds of sonication. This slurry was injected endotracheally into mice (5 mg/kg) using a 23-gauge needle. Twenty-one days after treatment, whole lung was homogenized in PBS supplemented with proteinase inhibitor (Roche Diagnostics) for analysis of type I collagen content by Western blotting. All animal studies were reviewed and approved by the University Committee on Use and Care of Animals at the University of Michigan.

Isolation of lung fibroblasts. Fibroblasts were isolated from isolated lung tissue by trypsinization as described previously (54). The cells were cultured in DMEM supplemented with 10% plasma-derived fetal bovine serum (PDS), 10 ng/ml EGF, and 5 ng/ml PDGF (R&D Systems Inc.). Cells were passaged by trypsinization and used at the third to fifth passage after primary culture. After plating as indicated, the cells were allowed to grow until they were 85% confluent before being used in the indicated experiments.

mRNA analysis by quantitative RT-PCR. For quantitative mRNA analysis, total RNA was isolated from lung tissue or fibroblasts. Primer Express 2.0 software (Applied Biosystems) was used to design TaqMan primers and MGB probes (6-FAM conjugated) for α-SMA, which were then purchased from Applied Biosystems. The primer and probe sequences for α-SMA were as follows: forward, 5′-CAACAGGATGAAGACTGCAACCT-3′; reverse, 5′-GGGACCATCAGCTAAAGAAG-3′; probe, 5′-6FAM-CCCTTCTCATCT-GCGTCT-3′. Primers and probe for GAPDH were purchased from Applied Biosystems. For each assay, 100 ng total RNA was used as template. GAPDH mRNA was used as internal control to normalize the amount of input RNA. One-step real-time RT-PCR (48°C for 30 minutes, 95°C for 10 seconds, followed by 45 cycles of 95°C for 10 seconds and 60°C for 1 minutes) was performed with TaqMan One Step RT-PCR Master Mix (Applied Biosystems) using a GeneAmp 7500 Sequence Detection System (Applied Biosystems). Results were expressed as $2^{-\Delta\Delta CT}$ as previously described (56).

Western blotting analysis. Western blotting to detect α-SMA and type I collagen protein expressions were performed as previously described (57). Briefly, 5 μg (α-SMA) and 50 μg (type I collagen) of cell extract proteins were loaded and separated by 12% and 8% SDS-PAGE, respectively. Mouse anti–α-SMA (Sigma-Aldrich) and rabbit anti–type I collagen (Biodesign International) antibodies were used as primary antibodies, and HRP-labeled anti-mouse and anti-rabbit IgG (Amersham Biosciences) were used as secondary antibodies. The immunostained bands were visualized using a chemiluminescent substrate (Cell Signaling Technology) followed by exposure to ECL Hyperfilm (Amersham Biosciences). The films were then scanned and quantitated using 1D Image Analysis software (Kodak).

Telomerase activity assay (TRAP-based ELISA). Telomerase activity was assayed using a telomerase PCR ELISA kit (Roche) in accordance with the manufacturer's protocols. Briefly, cell extracts were prepared by lysing the cultured fibroblasts with ice-cold lysis reagent. The protein concentrations were determined by the method of Bradford reagent (Bio-Rad Laboratories) and stored at –80°C until assayed. For each sample, 0.5 μg total cell protein was added to 25 μl reaction mixture containing telomerase substrate, including the biotin-labeled P1-TS and P2 primers, as well as nucleotides, Taq polymerase, and sterile water to a final volume of 50 μl. These mixtures were transferred to a PTC-200 DNA Engine thermal cycler (MJ research Inc.) for primer elongation at 25°C for 25 minutes, telomerase inactivation at 94°C for 5 minutes, and 30 cycles of amplification (94°C for 30 seconds, 50°C for 30 seconds, and 72°C for 90 seconds). Heat treatment of the cell extracts at 80°C for 10 minutes prior to the TRAP reaction was used as negative control. The positive control (human kidney 293 cells) was supplied by the assay kit. The PCR product (5 μl) was denatured and hybridized to a digoxigenin-labeled telomeric repeat–specific probe on the precoated microtiter plates at 37°C for 2 hours with shaking (300 rpm). Finally, anti-digoxigenin peroxidase conjugate and TMB substrate were used for ELISA assay, and the absorbance at 450 nm (with a reference wave length of 630 nm) was measured using an ELx 800 UV universal microplate reader (Bio-Tek Instruments Inc.). Based on the negative controls, samples with absorbance values less than 0.25 were considered negative.

HYP assay. Lung collagen deposition was estimated by measuring the HYP content of whole-lung homogenates as previously described (58). Briefly, the lungs were excised, homogenized in 0.5 M acetic acid, and hydrolyzed in 6N HCl overnight at 110°C. HYP was assessed by colorimetric assay, and the results were expressed as μg HYP per lung.

Cell proliferation assay. Isolated fibroblasts from BLM- and saline-treated TERT$^{-/-}$ and WT mice (cultured in DMEM supplemented with 10% PDS, 10 ng/ml EGF, and 5 ng/ml PDGF) were passaged once and then plated into 96-well plate at a density of 1×10^4 cells/well in a final volume of 100 μl medium. When the cells reached approximately 85% confluency on the next day, 10 μl WST-1 reagent (1:10 final dilution, WST-1 Cell Proliferation Kit II; Roche) was added to each well. After an additional 4 hours of incubation, cell proliferation was determined by measuring

the absorbance at 450 nm with reference wavelength of 690 nm using an ELx 800 UV Universal microplate reader. Only absorbance readings in the linear range (0.4–1.5) were used. The cells treated with 10 ng/ml PDGF were used as positive controls.

Induction and detection of cell apoptosis. The fibroblasts were plated into 4-well chamber slides (Nalge Nunc International), with a cell density of 5×10^3 cells/well, and allowed to reach subconfluence. Serum deprivation was achieved by maintenance in DMEM with 0.5% PDS for 24 hours. Apoptosis was induced by treating cells with 5 ng/ml TNF-α (R&D Systems) and 500 ng/ml CHX (Sigma-Aldrich) for 4 hours. Apoptosis was evaluated using TUNEL assay for in situ detection of apoptotic cells using the ApopTag Plus Fluorescein In Situ Apoptosis Detection Kit (Chemicon). After induction of apoptosis, cells were washed with PBS, fixed with 1% paraformaldehyde for 10 minutes at room temperature, and labeled by TUNEL in accordance with the manufacturer's protocol. Briefly, after fixation, cells were labeled for 60 minutes at 37°C using terminal deoxynucleotidyl transferase. The reaction was terminated in stop/wash buffer for 10 minutes at room temperature. The cells were then incubated with an anti-digoxigenin conjugate for 30 minutes at room temperature. Nuclei were labeled with PI. The cells were observed under a fluorescence microscope. For each slide, the number of positive cells were counted in randomly chosen, noncontiguous, high-power fields (original magnification, ×400) until a minimum of 500 total cells was counted.

Additionally, annexin V–FITC–PI staining (TACS annexin V–FITC; R&D Systems) was performed for early apoptosis detection. Briefly, the mouse lung fibroblasts were plated in 60-mm dishes with a cell density of 5×10^5 cells/dish. The cell were treated as described above with TNF-α and CHX for 4 hours and then collected after trypsinization, washed with ice-cold PBS, resuspended in 100 μl annexin V incubation reagent (10 μl 10× binding buffer, 10 μl PI, 1 μl annexin V–FITC, and 79 μl dH_2O) at a concentration of $3–5 \times 10^5$ cells/100 μl, and incubated for 15 minutes at room temperature in the dark. Samples were washed with binding buffer and analyzed by FACSCalibur (BD). Apoptotic cells were identified as an annexin V–FITC–positive/PI-negative population.

Single-cell gel electrophoresis assay. Single and double DNA breaks were evaluated using the Comet assay (R&D Systems) in accordance with the manufacturer's manual. Briefly, fresh lung tissue was minced into small pieces in 1 ml ice-cold PBS (Ca^{++} and Mg^{++} free) and 20 mM EDTA and let stand for 5 minutes. Cell suspension was recovered and pelleted by centrifugation and resuspended at 1×10^5 cells/ml in ice-cold PBS. For analysis of primary cultured lung fibroblasts, the cells were scraped using a rubber policeman and then resuspended in ice-cold PBS at 1×10^5 cell/ml after centrifugation. The cells were combined with 1% molten low–melting point agarose at a ratio of 1:10 (v/v) and immediately pipetted onto a CometSlide. After further incubation in the dark to lyse the cells and unwind DNA, the slides were subjected to electrophoresis and then treated with SYBR green I for viewing the DNA under a fluorescence microscope (Nikon Eclipse E600; Diagnostic Instruments Inc.). The cells treated with 400 μM H_2O_2 for 30 minutes on ice were used as a positive control.

Generation of BM chimera mice. BM chimeras were prepared as previously described (30), with minor modifications. Donor BM cells were collected from femurs and tibias of WT and $TERT^{-/-}$ mice by aspiration and flushing. Recipient WT or $TERT^{-/-}$ mice were exposed to 2 doses of 5 Gy given 3 hours apart using a ^{137}Cs irradiator and then maintained on acidified water and autoclaved feed ad libitum. After irradiation, 4×10^6 BM cells from donor mice in a volume of 200 μl sterile PBS were injected into recipient mice retro-orbitally under anesthesia. Six weeks after durable BM engraftment had been established, pulmonary fibrosis was induced by endotracheal BLM injection as described above.

Statistics. All data were expressed as mean ± SEM unless otherwise indicated. Differences between means of various treatment and control groups were assessed for statistical significance by ANOVA followed by post-hoc analysis using Scheffé's test for comparison between any 2 groups. A P value less than 0.05 was considered significant.

Acknowledgments

The authors thank Lisa R. Riggs for excellent technical assistance. This work was supported by NIH grants HL28737, HL31963, HL52285, and HL77297 and an award from the Sandler Foundation to S.H. Phan.

Received for publication April 11, 2007, and accepted in revised form September 12, 2007.

Address correspondence to: Sem H. Phan, Department of Pathology, University of Michigan Medical School, Med. Sci. I, Room 4204, Box 0602, Ann Arbor, Michigan 48109-2200, USA. Phone: (734) 647-8153; Fax: (734) 615-2331; E-mail: shphan@umich.edu.

Myoung Ja Chung's present address is: Department of Pathology, Chonbuk National University Medical School, Jeonju, Republic of Korea.

1. Greider, C.W. 1996. Telomere length regulation. *Annu. Rev. Biochem.* **65**:337–365.
2. Counter, C.M., et al. 1998. Telomerase activity is restored in human cells by ectopic expression of hTERT (hEST2), the catalytic subunit of telomerase. *Oncogene.* **16**:1217–1222.
3. Feng, J., et al. 1995. The RNA component of human telomerase. *Science.* **269**:1236–1241.
4. Blasco, M.A., Gasser, S.M., and Lingner, J. 1999. Telomeres and telomerase. *Genes Dev.* **13**:2353–2359.
5. Koyanagi, Y., et al. 2000. Telomerase activity is down regulated via decreases in hTERT mRNA but not TEP1 mRNA or hTERC during the differentiation of leukemic cells. *Anticancer Res.* **20**:773–778.
6. Tahara, H., et al. 1999. Immuno-histochemical detection of human telomerase catalytic component, hTERT, in human colorectal tumor and non-tumor tissue sections. *Oncogene.* **18**:1561–1567.
7. Broccoli, D., Young, J.W., and de Lange, T. 1995. Telomerase activity in normal and malignant hematopoietic cells. *Proc. Natl. Acad. Sci. U. S. A.* **92**:9082–9086.
8. Harle-Bachor, C., and Boukamp, P. 1996. Telomerase activity in the regenerative basal layer of the epidermis inhuman skin and in immortal and carcinoma-derived skin keratinocytes. *Proc. Natl. Acad. Sci. U. S. A.* **93**:6476–6481.
9. Nozaki, Y., Liu, T., Hatano, K., Gharaee-Kermani, M., and Phan, S.H. 2000. Induction of telomerase activity in fibroblasts from bleomycin-injured lungs. *Am. J. Respir. Cell Mol. Biol.* **23**:460–465.
10. Liu, T., Nozaki, Y., and Phan, S.H. 2002. Regulation of telomerase activity in rat lung fibroblasts. *Am. J. Respir. Cell Mol. Biol.* **26**:534–540.
11. Liu, T., et al. 2006. Telomerase regulation of myofibroblast differentiation. *Am. J. Respir. Cell Mol. Biol.* **34**:625–633.
12. Greider, C.W. 1998. Telomerase activity, cell proliferation, and cancer. *Proc. Natl. Acad. Sci. U. S. A.* **95**:90–92.
13. Sarin, K.Y., et al. 2005. Conditional telomerase induction causes proliferation of hair follicle stem cells. *Nature.* **436**:1048–1052.
14. Haendeler, J., Hoffmann, J., Rahman, S., Zeiher, A.M., and Dimmeler, S. 2003. Regulation of telomerase activity and anti-apoptotic function by protein-protein interaction and phosphorylation. *FEBS Lett.* **536**:180–186.
15. Mukherjee Nee Chakraborty, S., et al. 2007. Curcumin-induced apoptosis in human leukemia cell HL-60 is associated with inhibition of telomerase activity. *Mol. Cell. Biochem.* **297**:31–39.
16. Zhang, X., Mar, V., Zhou, W., Harrington, L., and Robinson, M.O. 1999. Telomere shortening and apoptosis in telomerase-inhibited human tumor cells. *Genes Dev.* **13**:2388–2399.
17. Rosenberger, S., Thorey, I.S., Werner, S., and Boukamp, P. 2007. A novel regulator of telomerase: S100A8 mediates differentiation-dependent and calcium-induced inhibition of telomerase activity in the human epidermal keratinocyte line HaCaT. *J. Biol. Chem.* **282**:6126–6135.
18. Savoysky, E., et al. 1996. Down-regulation of telomerase activity is an early event in the differentiation of HL60 cells. *Biochem. Biophys. Res. Commun.* **226**:329–334.
19. Bickenbach, J.R., et al. 1998. Telomerase is not an epidermal stem cell marker and is downregulated by calcium. *J. Invest. Dermatol.* **111**:1045–1052.
20. Kapanci, Y., Desmouliere, A., Pache, J.C., Redard, M., and Gabbiani, G. 1995. Cytoskeletal protein modulation in pulmonary alveolar myofibroblasts

during idiopathic pulmonary fibrosis. Possible role of transforming growth factor beta and tumor necrosis factor alpha. *Am. J. Respir. Crit. Care Med.* **152**:2163–2169.
21. Kuhn, C., and McDonald, J.A. 1991. The roles of the myofibroblast in idiopathic pulmonary fibrosis. Ultrastructural and immunohistochemical features of sites of active extracellular matrix synthesis. *Am. J. Pathol.* **138**:1257–1265.
22. Mitchell, J., et al. 1989. Alpha-smooth muscle actin in parenchymal cells of bleomycin-injured rat lung. *Lab. Invest.* **60**:643–650.
23. Zhang, K., Rekhter, M.D., Gordon, D., and Phan, S.H. 1994. Myofibroblasts and their role in lung collagen gene expression during pulmonary fibrosis. A combined immunohistochemical and in situ hybridization study. *Am. J. Pathol.* **145**:114–125.
24. Kaminski, N. 2003. Microarray analysis of idiopathic pulmonary fibrosis. *Am. J. Respir. Cell Mol. Biol.* **29**:S32–S36.
25. King, T.E., Jr., et al. 2001. Idiopathic pulmonary fibrosis: relationship between histopathologic features and mortality. *Am. J. Respir. Crit. Care Med.* **164**:1025–1032.
26. Yuan, X., et al. 1999. Presence of telomeric G-strand tails in the telomerase catalytic subunit TERT knockout mice. *Genes Cells.* **4**:563–572.
27. Banner, S.H., Ruben, L.N., and Johnson, R.O. 2007. Bleomycin-induced DNA damage and repair in Xenopus laevis and Xenopus tropicalis. *J. Exp. Zool. Part A Ecol. Genet. Physiol.* **307**:84–90.
28. Rose, J.L., Reeves, K.C., Likhotvorik, R.I., and Hoyt, D.G. 2007. Base excision repair proteins are required for integrin-mediated suppression of bleomycin-induced DNA breakage in murine lung endothelial cells. *J. Pharmacol. Exp. Ther.* **321**:318–326.
29. Reynolds, R., Witherspoon, S., and Fox, T. 2004. The infant mouse as a in vivo model for the detection and study of DNA damage-induced changes in the liver. *Mol. Carcinog.* **40**:62–72.
30. Hashimoto, N., Jin, H., Liu, T., Chensue, S.W., and Phan, S.H. 2004. Bone marrow-derived progenitor cells in pulmonary fibrosis. *J. Clin. Invest.* **113**:243–252. doi:10.1172/JCI200418847.
31. Phan, S.H. 2002. The myofibroblast in pulmonary fibrosis. *Chest.* **122**:286S–289S.
32. Selman, M., King, T.E., and Pardo, A. 2001. Idiopathic pulmonary fibrosis: prevailing and evolving hypotheses about its pathogenesis and implications for therapy. *Ann. Intern. Med.* **134**:136–151.
33. Blasco, M.A. 2002. Telomerase beyond telomeres. *Nat. Rev. Cancer.* **2**:627–633.
34. Flores, I., Cayuela, M.L., and Blasco, M.A. 2005. Effects of telomerase and telomere length on epidermal stem cell behavior. *Science.* **309**:1253–1256.
35. Kraemer, K., et al. 2006. Microarray analyses in bladder cancer cells: inhibition of hTERT expression down-regulates EGFR. *Int. J. Cancer.* **119**:1276–1284.
36. Schissel, S.L., and Layne, M.D. 2006. Telomerase, myofibroblasts, and pulmonary fibrosis. *Am. J. Respir. Cell Mol. Biol.* **34**:520–522.
37. Blasco, M.A. 2005. Telomeres and human disease: ageing, cancer and beyond. *Nat. Rev. Genet.* **6**:611–622.
38. Gonzalez-Suarez, E., Samper, E., Flores, J.M., and Blasco, M.A. 2000. Telomerase-deficient mice with short telomeres are resistant to skin tumorigenesis. *Nat. Genet.* **26**:114–117.
39. Leri, A., et al. 2003. Ablation of telomerase and telomere loss leads to cardiac dilatation and heart failure associated with p53 upregulation. *EMBO J.* **22**:131–139.
40. Lee, H.W., et al. 1998. Essential role of mouse telomerase in highly proliferative organs. *Nature.* **392**:569–574.
41. Rudolph, K.L., et al. 1999. Longevity, stress response, and cancer in aging telomerase-deficient mice. *Cell.* **96**:701–712.
42. Rice, A.B., Moomaw, C.R., Morgan, D.L., and Bonner, J.C. 1999. Specific inhibitors of platelet-derived growth factor or epidermal growth factor receptor tyrosine kinase reduce pulmonary fibrosis in rats. *Am. J. Pathol.* **155**:213–221.
43. Brachner, A., et al. 2006. Telomerase- and alternative telomere lengthening-independent telomere stabilization in a metastasis-derived human non-small cell lung cancer cell line: effect of ectopic hTERT. *Cancer Res.* **66**:3584–3592.
44. de Lange, T. 2006. Lasker Laurels for telomerase. *Cell.* **126**:1017–1020.
45. Niida, H., et al. 1998. Severe growth defect in mouse cells lacking the telomerase RNA component. *Nat. Genet.* **19**:203–206.
46. Rebuzzini, P., Martinelli, P., Blasco, M., Giulotto, E., and Mondello, C. 2007. Inhibition of gene amplification in telomerase deficient immortalized mouse embryonic fibroblasts. *Carcinogenesis.* **28**:553–559.
47. Bodnar, A.G., et al. 1998. Extension of life-span by introduction of telomerase into normal human cells. *Science.* **279**:349–352.
48. Steinert, S., Shay, J.W., and Wright, W.E. 2000. Transient expression of human telomerase extends the life span of normal human fibroblasts. *Biochem. Biophys. Res. Commun.* **273**:1095–1098.
49. Kanzaki, Y., Onoue, F., Ishikawa, F., and Ide, T. 2002. Telomerase rescues the expression levels of keratinocyte growth factor and insulin-like growth factor-II in senescent human fibroblasts. *Exp. Cell Res.* **279**:321–329.
50. Armanios, M.Y., et al. 2007. Telomerase mutations in families with idiopathic pulmonary fibrosis. *N. Engl. J. Med.* **356**:1317–1326.
51. Tsakiri, K.D., et al. 2007. Adult-onset pulmonary fibrosis caused by mutations in telomerase. *Proc. Natl. Acad. Sci. U. S. A.* **104**:7552–7557.
52. McElligott, R., and Wellinger, R.J. 1997. The terminal DNA structure of mammalian chromosomes. *EMBO J.* **16**:3705–3714.
53. Dionne, I., and Wellinger, R.J. 1996. Cell cycle-regulated generation of single-stranded G-rich DNA in the absence of telomerase. *Proc. Natl. Acad. Sci. U. S. A.* **93**:13902–13907.
54. Phan, S.H., Varani, J., and Smith, D. 1985. Rat lung fibroblast collagen metabolism in bleomycin-induced pulmonary fibrosis. *J. Clin. Invest.* **76**:241–247.
55. Moore, B.B., et al. 2001. Protection from pulmonary fibrosis in the absence of CCR2 signaling. *J. Immunol.* **167**:4368–4377.
56. Livak, K.J., and Schmittgen, T.D. 2001. Analysis of relative gene expression data using real-time quantitative PCR and the 2(-Delta Delta C(T)) method. *Methods.* **25**:402–408.
57. Liu, T., et al. 2004. FIZZ1 stimulation of myofibroblast differentiation. *Am. J. Pathol.* **164**:1315–1326.
58. Huaux, F., Liu, T., McGarry, B., Ullenbruch, M., and Phan, S.H. 2003. Dual roles of IL-4 in lung injury and fibrosis. *J. Immunol.* **170**:2083–2092.